pubs.acs.org/Biomac

Article

Inhibition of Herpes Simplex Virus Type 1 Attachment and Infection by Sulfated Polyglycerols with Different Architectures

Paria Pouyan, Chuanxiong Nie, Sumati Bhatia, Stefanie Wedepohl, Katharina Achazi, Nikolaus Osterrieder, and Rainer Haag*

Cite This: *Biomacromolecules* 2021, 22, 1545−1554

Read Online

ACCESS | Metrics & More | Article Recommendations | Supporting Information

ABSTRACT: Inhibition of herpes simplex virus type 1 (HSV-1) binding to the host cell surface by highly sulfated architectures is among the promising strategies to prevent virus entry and infection. However, the structural flexibility of multivalent inhibitors plays a major role in effective blockage and inhibition of virus receptors. In this study, we demonstrate the inhibitory effect of a polymer scaffold on the HSV-1 infection by using highly sulfated polyglycerols with different architectures (linear, dendronized, and hyperbranched). IC_{50} values for all synthesized sulfated polyglycerols and the natural sulfated polymer heparin were determined using plaque reduction infection assays. Interestingly, an increase in the IC_{50} value from 0.03 to 374 nM from highly flexible linear polyglycerol sulfate (LPGS) to less flexible scaffolds, namely, dendronized polyglycerol sulfate and hyperbranched polyglycerol sulfate was observed. The most potent LPGS inhibits HSV-1 infection 295 times more efficiently than heparin, and we show that LPGS has a much reduced anticoagulant capacity when compared to heparin as evidenced by measuring the activated partial thromboplastin time. Furthermore, prevention of infection by LPGS and the commercially available drug acyclovir were compared. All tested sulfated polymers do not show any cytotoxicity at concentrations of up to 1 mg/mL in different cell lines. We conclude from our results that more flexible polyglycerol sulfates are superior to less flexible sulfated polymers with respect to inhibition of HSV-1 infection and may constitute an alternative to the current antiviral treatments of this ubiquitous pathogen.

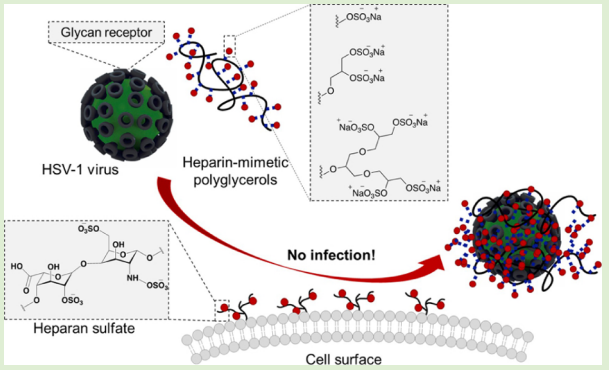

INTRODUCTION

Herpes simplex virus type 1 (HSV-1) is one of the eight human herpes viruses and among the most widespread viruses in the human population with an estimation of 60−90% seropositivity among adults worldwide.[1] HSV-1 is an enveloped spherical virus with a diameter of 155−240 nm which harbors a double-stranded DNA in the capsid, which can infect the host tissue through the epithelial cells of the mucosal membrane. The virus is known to establish a lifelong infection in the sensory neurons of the host, out of which it can periodically recrudesce by different stimuli such as stress, local trauma, or specific bacterial infections.[1−3] HSV-1 often causes oral and pharyngeal infection, while its close relative, HSV-2, primarily targets the genital tract.[4] Although HSV-1 infection is usually mild and locally confined, HSV-1 is the main cause of encephalitis in newborns and immunocompromised patients,[5] and recent studies suggest a role of HSV-1 infection in dementia and neurodegenerative diseases like Alzheimer's disease.[6] At the late stages of infection, it can lead to keratitis or permanent infectious blindness.[7,8]

The major antiviral drugs to treat HSV-1 and other herpesvirus infections are acyclic nucleosides like acyclovir (ACV) and ganciclovir, which can inhibit viral DNA replication.[2,9] Although these nucleoside analogues have been shown to be useful for reducing symptoms of infection and slowing down the virus spread, their application is limited because of their poor water solubility, low bioavailability, and low tissue permeability. Also, side effects like dizziness, confusion, weakness, and nausea in some patients render its application challenging.[2] Frequent prescription of ACV against HSV infections for the past 40 years has also led to the emergence of virus mutants that are resistant to the drugs.[9,10] Finding alternative ways to intervene with HSV viral infections is therefore of priority, especially for topical applications.

Inhibiting virus entry into the host cells at the early stage of infection is one promising concept of infection prevention and treatment.[11] HSV-1 entry into the cell is driven by two types of

Received: December 21, 2020
Revised: February 18, 2021
Published: March 12, 2021

https://dx.doi.org/10.1021/acs.biomac.0c01789
Biomacromolecules 2021, 22, 1545−1554

interactions. First, electrostatic interactions occur between the negatively charged heparan sulfates (HSs) present on the host cell surface and the positively charged virion surface.[12] Second, glycoproteins B and C (gB and gC) present in the virus envelope specifically bind to HS on the plasma membrane of the host cell.[13,14] HS is among the highly negatively charged biopolymers and is abundant on the cell surface of most of the cells.[15]

The knowledge of the early interaction of HSV-1 with the host cell has led to exploring cationically modified polysaccharides such as dextran derivatives modified with quaternary ammonium groups[16] and block copolymers with a cationic block of trimethylammonium groups for the prevention of HSV-1 infection.[17] However, typically, polycations exhibit relatively high cytotoxicity, which restricts their widespread application in humans.[18]

Decoying polymeric scaffolds with carboxylate and carboxylic acid moieties have been shown to introduce antiviral activity by inhibiting the viral entry to the host cells.[19,20] It has been shown that the FDA-approved cellulose acetate phthalate in the regular and nanoparticle (NP) form has selectivity and antiviral activity against HSV types 1 and 2, although their exact mechanism of action is under further investigation.[21]

Negatively charged polysaccharides, with similar structures to HS like heparin, have been used as binding decoys to prevent HSV-1 infection.[22,23] However, clinical application of heparin as an antiherpetic drug is limited because of its heterogeneity and possible impurities.[23] Also, its anticoagulant activity can induce undesired side effects, including bleeding.[24] Therefore, the development of negatively charged synthetic polymers with anti-HSV-1 activity is of high interest.

Inspired by HS on the cell surface and heparin, sulfated polymers, so-called heparin mimetics, have been developed and have characteristics similar to HS.[25] Counterion release is the main driving force for the polyelectrolyte (i.e., HS, heparin, or heparin mimetics) interactions with the virus in the way that patches of positive charge of the virus surface (gB and gC) act as multivalent counterions of the highly negatively charged polymer and lead to a favorable increase in entropy by the release of counterions from the polyelectrolyte.[26] Synthetic sulfated glycomimetic polymers were shown to have a broad-spectrum antiviral activity while also having a homogeneous structure.[11] However, synthesis and modification of such polymers is challenging. Low cytotoxicity and efficient in vivo clearance of polyglycerol (PG) make them a promising candidate for biological applications.[27,28] Hyperbranched polyglycerol sulfate (hPGS) has been reported earlier by our group to exhibit anti-inflammatory activities that are similar to those of heparin.[29,30] Furthermore, dPGS-conjugated graphene oxide (GO) scaffolds were shown to inhibit the HSV-1 infection.[31−33] Furthermore, sulfated PG-based nanogels with different flexibilities were investigated for their antiviral activity against HSV-1 where more flexible nanogels exhibited robust and broad antiviral activities against such viruses. In another study, more flexible sialylated nanogels also showed better inhibition of influenza A virus than the less flexible structures.[34] These studies signify the importance of scaffold flexibility for virus inhibition. However, large size and high molecular weight scaffolds are not recommended for clinical development because of clearance and degradation issues.

In this study, we introduce low molecular weight (≤40 kDa) and highly biocompatible linear PG-based heparin-mimetic scaffolds with different structures and flexibilities as efficient antiviral agents against HSV-1 infection. The synthesized polymers include a flexible linear polyglycerol sulfate (LPGS) and two dendronized polyglycerol sulfates (DenPGSs) each carrying a $G_{0.5}$ ($DenPG_{0.5}S$) or G_1 ($DenPG_1S$) glycerol dendron on each repeating unit, introducing different flexibilities to the polymeric backbone which are induced by steric hindrance. These novel structures were first tested for their cell compatibility, and then the effect of their structural flexibility on virus inhibition properties was tested in pre- and postinfection assays against HSV-1 in comparison to hPGS, which has a globular and hence less flexible structure than the linear ones, and commercially available heparin as a standard HSV-1 inhibitor. To the best of our knowledge, this is the first report on sulfated linear and DenPGSs for the virus inhibition.

MATERIALS AND METHODS

Materials. Anhydrous solvents (dimethylformamide and toluene), benzoylated cellulose dialysis tubes (2000 kDa, 32 mm width), and heparin (sodium salt from porcine intestinal mucosa, H3393-500KU) were purchased from Merck (Darmstadt, Germany). Acetal-protected generation 1 dendrons were synthesized in our group according to a published procedure.[35] Tetra-*n*-octyl ammonium bromide 98% was purchased from ACROS Organics and used as received. All other chemicals were bought from Merck (Darmstadt, Germany) unless stated otherwise. Elemental composition determination was performed on a Vario EL CHNS element analyzer by Elementar Analysensysteme GmbH (Langenselbold, Germany). ^{1}H NMR spectra were recorded on a Bruker AMX 500 (Bruker Corporation) or JEOL ECP 500 (JEOL GmbH). Chemical shifts (δ) are reported in ppm via the deuterated solvent peak as the standard. IR measurements were done on a Nicolet AVATAR 320 FT_IR 5 SXC (Thermo Fisher Scientific) with a detector range of 4000−650 cm^{-1}. Gel permeation chromatography (GPC) measurements in water were performed with an Agilent 1100 equipped with an automatic injector, isopump, and Agilent 1100 differential refractometer (Agilent Technologies, Santa Clara, CA, USA). The PSS Suprema (pre-column), 1× with pore size of 30 Å, 2× with pore size of 1000 Å (all of them with a particle size of 10 μm) column, was calibrated against Pullulan standards prior to measurements. The GPC measurements in tetrahydrofuran (THF) were done with an Agilent SECurity (1200 Serie), equipped with an automatic injector, isopump, and UV and RI detector. The separation was done via a photoluminescence gel from Agilent (1× pre-column, 3× Mixed-C with a particle size of 5 μm), which was calibrated against polystyrene standards.

Synthesis of Ethoxyethyl Glycidyl Ether 2. The acetal protection of glycidol was carried out with slight modifications to a reported protocol.[36] In summary, in an ice bath, glycidol (70 mL, 1.052 mol, 1 eq) was mixed under stirring with divinyl ether (403.3 mL, 4.21 mol, 4 eq), and *p*-TsOH·H_2O (2 g, 0.0105 mol, 0.01 eq) was slowly added to the mixture. After 4 h, the reaction was quenched and washed with saturated $NaHCO_3$ solution. The organic phase was dried over sodium sulfate and concentrated under reduced pressure. The crude product was dried over CaH_2 and distilled under vacuum over a preheated molecular sieve and stored under argon in a freezer until further use. Because of storage under dry and inert conditions, weighing of the final product was not possible and a complete conversion of the starting material is assumed.

^{1}H NMR (500 MHz, Acetone-d_6): δ 4.70 (t, J = 5.3, 2.4 Hz, 1H), 3.77 (m, 1H), 3.73−3.57 (m, 1H), 3.50−3.41 (m, 1H), 3.30 (dd, J = 11.5, 6.4 Hz, 1H), 3.12−3.00 (m, 1H), 2.74−2.66 (m, 1H), 2.52 (m, 1H), 1.22 (t, J = 5.3 Hz, 3H), 1.12 (td, J = 7.1, 1.1 Hz, 3H). ^{13}C NMR (500 MHz, Acetone-d_6): δ 100.49 (tertiary CH acetal), 67.25 (CH_2), 66.61 (CH_2 acetal), 61.42 (CH epoxide), 44.47 (CH_2 epoxide), 20.29 (CH_3 acetal), 15.83 (CH_3 acetal).

Synthesis of 1,2-Isopropylidene Glyceryl Glycidyl Ether 6. The synthesis was carried out according to a reported protocol.[37] In summary, solketal (1,2-isopropylideneglycerol) (12 g, 0.151 mol, 1 eq) was dissolved in 20 mL of toluene and 20 mL of 50% NaOH.

https://dx.doi.org/10.1021/acs.biomac.0c01789
Biomacromolecules 2021, 22, 1545−1554

TBAB (4.86 g, 0.0151 mol, 0.1 eq) was added, and the mixture was cooled down to 10 °C and epichlorohydrin (70 mL, 0.755 mol, 5 eq) was added slowly to the mixture. The mixture was stirred for 48 h at room temperature, diluted with diethylether, and washed with saturated $NaHCO_3$, NaCl, and water. The organic phase was dried over $MgSO_4$. After concentration under vacuum, the product was obtained as a colorless liquid and was stored over dried molecular sieve before polymerization (yield 82%).

^{1}H NMR (500 MHz, Methanol-d_4): δ 4.24 (m, 1H), 4.10−3.97 (m, 1H), 3.80 (dt, J = 11.7, 2.3 Hz, 1H), 3.73−3.65 (m, 1H), 3.53 (m, 1H), 3.16−3.07 (m, 1H), 2.75 (m, 1H), 2.57 (dd, J = 5.1, 2.7 Hz, 1H), 1.36 (s, 3H), 1.31 (s, 3H). ^{13}C NMR (500 MHz, Methanol-d_4): δ 109.23 (quaternary C acetal), 76.16 (CH acetal), 74.85 (CH_2 acetal), 66.28 (CH_2),51.24 (CH epoxide), 43.31 (CH_2 epoxide), 25.82 (CH_3 acetal), 24.46 (CH_3 acetal). ESI-MS: $[M + Na]^+$: 211.09 (theoretical), 211.09 (observed).

Modification of First-Generation Glycerol Dendrons with Epoxide 10. The synthesis was carried out similar to isopropylidene glyceryl glycidyl ether (IGG) synthesis. G_1-dendrons (10.5 g, 0.032 mol, 1 eq) were dissolved in a mixture of 17 mL of toluene and 17 mL of 50% NaOH. TBAB (2.11 g, 0.006 mol, 0.2 eq) was added, and the mixture was cooled down to 10 °C. Epichlorohydrin (13 mL, 0.165 mol, 7 eq) was added dropwise, and the mixture was left to stir for 48 h. The reaction was diluted with diethylether and was extracted three times with saturated $NaHCO_3$, NaCl, and water. The organic phase was separated and dried with $MgSO_4$. The product was purified with flash chromatography (85% cyclohexan, 15% ethylacetate) (yield 70%). The product was dried over activated molecular sieve before polymerization. ^{1}H NMR (500 MHz, Methanol-d_4): δ 4.25 (m, 2H), 4.05 (dd, J = 8.3, 6.5 Hz, 2H), 3.91 (dd, J = 11.8, 2.7 Hz, 1H), 3.76−3.66 (m, 3H), 3.64−3.46 (m, 9H), 3.16−3.12 (m, 1H), 2.76 (dd, J = 5.1, 4.2 Hz, 1H), 2.61 (m, 1H), 1.38 (t, J = 0.7 Hz, 6H), 1.33 (d, J = 1.0 Hz, 6H). ^{13}C NMR (500 MHz, Methanol-d_4): δ 110.39 (quaternary C acetal), 79.60 (tertiary CH, G1), 76.06 (tertiary CH, acetal), 73.34 (CH_2), 72.40 (CH_2 acetal), 67.51(CH_2 arms), 52.02 (CH epoxide), 44.72 (CH_2 epoxide), 27.08 (CH_3 acetal), 25.69 (CH_3 acetal). ESI-MS: $[M + Na]^+$: 399.43 (theoretical), 399.20 (observed), $[M + K]^+$: 415.54 (theoretical), 415.18 (observed).

All the polymerizations were done according to a reported protocol for monomer-activated ring-opening polymerization.[36]

Polymerization of Ethoxyethyl Glycidyl Ether. In a flame-dried Schlenck flask, Oct_4NBr (172.78 mg, 0.310 mmol, 0.0047 eq) was dried under high vacuum and dissolved in 60 mL of dry toluene. Afterward, ethoxyethyl glycidyl ether (10 mL, 65.6 mmol, 1 eq) was added under an argon atmosphere to the solution to afford 200 repeating units per chain. The mixture was cooled down in an ice bath to 0 °C, and i-Bu_3Al (1.4 mL, 1.55 mmol, 0.023 eq) was added all at once under an argon atmosphere and brisk stirring. The reaction was left to proceed overnight, which was quenched by the addition of 1 mL of ethanol. The crude product was dissolved in cold Et_2O to precipitate the excess i-Bu_3Al. The product was dialyzed in acetone (MWCO: 2 kDa) for further purification. After drying, the product was obtained as 8.38 g colorless viscous oil (50%). (GPC THF-$\overline{M_n}$: 32.4 kDa, PDI: 1.07). ^{1}H NMR (500 MHz, Acetone-d_6): δ 4.81−4.60 (m, 1H), 3.83−3.32 (m, 7H, monomer unit), 1.33−1.22 (m, 3H), 1.14 (t, J = 7.1 Hz, 3H). ^{13}C NMR (500 MHz, Acetone-d_6): δ 102.69 (tertiary CH acetal), 79.12 (CH backbone), 70.24 (CH_2), 65.19 (CH_2 backbone), 62.37 (CH_2 acetal), 19.55 (CH_3 acetal), 15.03 (CH_3 acetal).

Polymerization of 1,2-IGG (DenPG$_{0.5}$). In a flame-dried Schlenk flask, N(Oct)$_4$Br (50.2 mg, 0.089 eq, 0.09 mmol) was dried by melting and flushed with argon. After cooling down, the salt was solved in 11 mL of dry toluene. Thereafter, the monomer (1.8 mL, 11.3 mmol, 1 eq) was added to afford 100 repeating units per chain and the mixture was cooled down to 0 °C. Then, i-Bu_3Al (0.4 mL of 1.1 M stock solution) was added all at once under brisk stirring. The reaction was allowed to run overnight and was quenched by the addition of 1 mL of ethanol and concentrated under vacuum. The activator was precipitated in cold Et_2O and dialyzed in acetone (MWCO: 2 kDa) for further purification. The product was obtained as viscous clear oil (yield 90%). (GPC THF-$\overline{M_n}$: 23.5 kDa, PDI: 1.13). ^{1}H NMR (500 MHz, Methanol-d_4): δ 4.26 (m, 2H), 4.07 (dd, J = 8.2, 6.4 Hz, 2H), 3.87−3.44 (br, 6H), 1.40 (s, 3H), 1.35 (s, 3H). ^{13}C NMR (500 MHz, Methanol-d_4) δ 110.45 (CH acetal), 76.12 (CH backbone, CH acetal), 72.76 (CH_2), 71.11 (CH_2), 67.86 (CH_2 backbone, CH_2 acetal), 27.42 (CH_3 acetal), 25.98 (CH_3 acetal).

Polymerization of First-Generation Glycerol Dendrons with Epoxide. In a flame-dried 50 mL Schlenk flask, N(Oct)$_4$Br (50.4 mg, 0.092 mmol, 0.017 eq) was dried by melting and flushed with argon. After cooling down, the salt was dissolved in 12 mL of dry toluene. Thereafter, the monomer (2 mL, 5.3 mmol, 1 eq) was added to afford 50 repeating units per chain, and the mixture was cooled down to 0 °C. Then (1.23 mL of 1.1 M stock solution), i-Bu3Al was added all at once under brisk stirring. The reaction was allowed to run over night and was quenched by the addition of 1 mL of water. Then, the mixture was dried with $MgSO_4$, filtered, and concentrated under vacuum. The mixture was precipitated in cold diethylether and dialyzed in acetone with a 2 kDa MWCO membrane for further purification. The product was obtained as viscous clear oil (yield 93%). (GPC THF-$\overline{M_n}$: 19.34 kDa, PDI: 1.21). ^{1}H NMR (500 MHz, Methanol-d_4): δ 4.25 (m, 2 H), 4.05 (m, 2H), 3.81−3.71 (m, 3H), 3.65−3.45 (m, 9H), 1.38 (m, 6H), 1.33 (m, 6H). ^{13}C NMR (500 MHz, Methanol-d_4): δ 109.13 (quaternary C acetal), 78.46(tertiary CH, G1), 74.79 (tertiary CH, acetal), 71.16 (CH_2 acetal), 66.56 (CH_2 arms), 26.17 (CH_3 acetal), 24.75 (CH_3 acetal).

Deprotection of Acetal-Protected PGs 3, 7, 11. The respective polymers were dissolved in ethanol (1 g in 10 mL), and then HCl 37% (3% of the ethanol) was added to the solution. The mixture was left to stir overnight and dialyzed in water (MWCO: 2 kDa) for 2 days to afford the desired polymers in quantitative yields.

Sulfation of the PGs. All polymers were sulfated according to an already published protocol.[29] The completely dry corresponding polymer was dissolved in dry dimethylformamide (10 mL for 1 g). The mixture was then heated up to 60 °C, and a respective amount of SO_3/pyridine (1.5 eq of −OH groups) was added to it. The reaction was allowed to run overnight. Thereafter, the pH was brought to 9 by the addition of 1 M NaOH to the solution. Then, the polymer was dialyzed against saturated solution of NaCl for 2 days and 2 days in water. After drying in high vacuum, the crude product was obtained as a white solid powder. The degree of functionalization was determined via elemental analysis.

Used cell lines and cell cultivation conditions: For the different cell-based assays and tests used in this publication, cells were routinely maintained at 37 °C and 5% CO_2 and passaged every 3−4 days after reaching 70 to 90% confluency or before being used for a test or assay. A549 human lung carcinoma cells (DSMZ ACC 107) and Vero E6 African green monkey kidney epithelial cells (ATCC CRL-1586) were cultured in Dulbecco's Modified Eagle Medium (DMEM), while 16HBE14o human bronchial epithelial cells (Millipore SCC150) were cultivated in minimum essential media all supplemented with 10% fetal bovine serum, penicillin/streptomycin, and glutamine (all from Gibco BRL, Eggenstein, Germany). Cells were routinely tested for the absence of mycoplasma by a published PCR test protocol using the primer pair MGSO-(TGCACCATCTGTCACTCTGTTAACCTC-3′) and GPO-3 (5′- GGGAGCAAACAGGATTAGATACCCT-3′).[38]

Cell Viability Assay CCK-8. To analyze the cytotoxicity and determine the half-maximal cytotoxic concentration (CC_{50}) of compounds, the cell viability assay Cell Counting Kit 8 (CCK-8) from Sigma-Aldrich Chemie GmbH (Taufkirchen, Germany) was used according to the manufacturer's instructions. In short, A549, Vero E6 16HBE14o cells were cultivated as described above and seeded 24 h prior to the compound treatment in all inner wells of a 96-well plate (4.000 cells/well); in all outer wells, the same cell culture medium as used for the respective seeded cell line without cells was added. After an overnight incubation, compounds were added in serial dilutions in triplicates to the wells containing cells and additionally in one outer well without cells for subsequent background subtraction. Sodium dodecyl sulfate (1%) and the nontreated cells served as a control. The 96-well plates were incubated for another day

https://dx.doi.org/10.1021/acs.biomac.0c01789
Biomacromolecules 2021, 22, 1545−1554

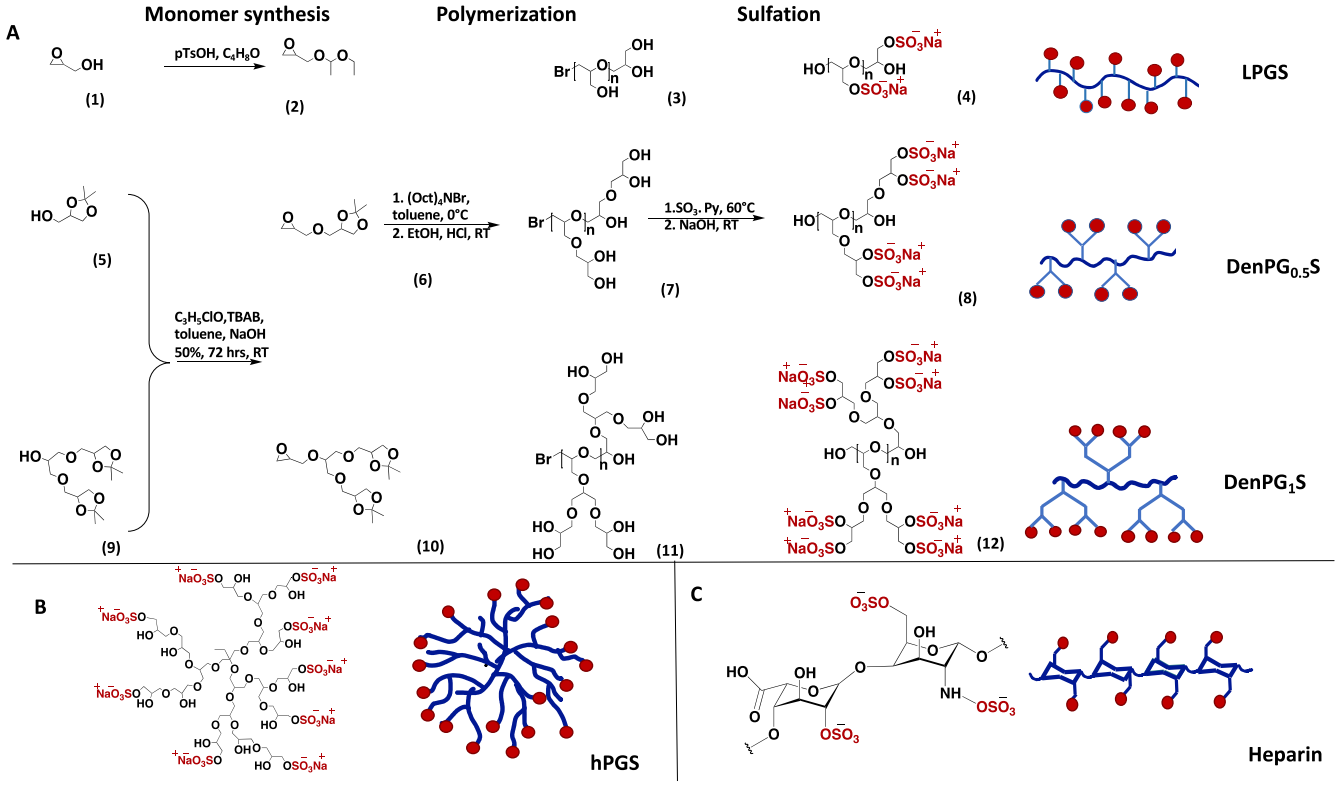

Figure 1. Overview of the synthesis and cartoon representation of used structures. (A) Monomer synthesis, polymerization, and sulfation of PGs, (B) structure of hPGS, and (C) structure of heparin.

at 37 °C before the CCK-8 solution was applied for approximately 2 h. The 96-well plate was transferred to a microplate reader (TECAN Infinite M200 Pro, Tecan Group Ltd., Männedorf, Switzerland) and absorbance was measured at a measurement wavelength of 450 nm and a reference wavelength of 650 nm. For each cell line and compound, the assay was repeated in three test rounds. To calculate the cell viability after treatment, the background was subtracted in each test round for each replicate, compound, and concentration using the respective wells without cells. Then, the nontreated control was set to 100% to calculate the cell viability in percent for each compound concentration and controls for each test round by a standard excel sheet. GraphPad Prism software (GraphPad Prism 6 for Windows, Version 6.01) was used to summarize values for all three test rounds ($n = 3$) and to calculate the CC_{50} using the "log(inhibitor) vs normalized response" equation. Data is presented as mean cell viability with standard deviation.

Virus Propagation and Virus Titer Determination. The GFP-tagged HSV-1[33] (kindly provided by Dr. Yasushi Kawaguchi, University of Tokyo, Japan) was propagated on Vero E6 cells (ATCC CRL-1586) for 2 days. The supernatant containing GFP-tagged HSV-1 virus was collected, and the number of infectious virus particles (virus titer) in the supernatant was assessed using a plaque assay. For the plaque assay, Vero E6 cells were preseeded in a 12-well plate for 2 days before adding 200 μL of virus-containing solution for 45 min. Afterward, 1 mL of 0.5% methylcellulose (Sigma M0262) was added to the wells as an overlay medium. Cells were cultured for 2 days with the overlay medium so that virus transmission can only occur from cell to cell but not through the cell culture medium. As a result, one cell initially infected by one virus particle over time causes the infection of the surrounding cells that all together can be visualized as one so-called plaque. The number of plaques per well was assessed using an epifluorescence microscope (Zeiss AxioVert 100) using the GFP channel and the virus titer of the initially added solution was calculated and is expressed as plaque-forming units (PFU)/mL.

Plaque Reduction Assay. For assessing the potential of the compounds to prevent infection, a plaque reduction assay was performed. For the plaque reduction assay, Vero E6 cells were preseeded in a 12-well plate to confluency. 10-fold dilution series of the compounds in 100 μL of DMEM down to 0.1 ng/mL were prepared, and each dilution was incubated with 100 μL of virus solution containing GFP-expressing HSV-1 (2000 PFU/mL) for 45 min at 37 °C. Afterward, the infectivity of the mixture was titrated by a plaque assay using Vero E6 cells as described above. The inhibition of the HSV-1 infection in Vero E6 cells is calculated as follows

$$\text{Inhibition (\%)} = \left(1 - \frac{\text{Plaque number(sample)}}{\text{Plaque number(virus control)}}\right) \times 100\%$$

The respective half-maximal inhibitory concentration (IC_{50}) of each compound was estimated by using the software GraphPad Prism 7 and applying the dose−response model. The tests were done three times with individual experiments.

Multicycle virus replication inhibition: For the postinfection inhibition assays, preseeded Vero E6 cells (80% confluency in a 24-well plate) were infected by HSV-1_GFP at a multiplicity of infection (MOI) of 0.1. At 1 h postinfection (p.i.), the compounds were added into the cell culture medium to a final concentration of 100 μg/mL. After 24 h, the cells were fixed by 2.5% formaldehyde and stained by DAPI to examine the infection by fluorescence microscopy (Zeiss AxioVert 100); the number of infectious viral particles in the supernatants was assessed by plaque assays as described above. For the preinfection assay, the preseeded Vero E6 cells were treated first with the compounds at 37 °C for 1 h and before adding HSV-1_GFP containing solution at a MOI of 0.1. The cellular infection and the number of infectious virus particles in the supernatant were assessed after 24 h as described for the postinfection assay.

Activated Partial Thrombosis Time. Samples were dissolved in Milli-Q (MQ) water to a concentration of 10 mg/mL; 5 μL of these solutions was diluted serially with water to give the desired concentrations. $CaCl_2$ was placed into the warming area of the coagulometer (STart Max, Stago) and prewarmed at 37 °C for at least

https://dx.doi.org/10.1021/acs.biomac.0c01789
Biomacromolecules 2021, 22, 1545−1554

Table 1. Overview of Inhibitors and Their Characterization

sample	$\overline{M}_n$(kDa)	PDI[a]	degree of sulfation[b] (%)	ζ-potential (mV)	CC_{50} (mg/mL)	IC_{50} (μg/mL)[c]	IC_{50} (nM)
LPGS	17.7[a]	1.2	94	−26.13 ± 0.71	>1	0.0016 ± 0.0005	0.03
$DenPG_{0.5}S$	18.7[a]	1.2	88	−25.46 ± 3.31	>1	0.049 ± 0.009	1.52
$DenPG_1S$	14.6[a]	1.6	94	−31.87 ± 1.29	>1	0.072 ± 0.021	3.53
hPGS	9.1[a]	1.3	91	−22.63 ± 0.51	>1	3.405 ± 1.14	374.17
heparin	13−15			−20.05 ± 4.25		0.124 ± 0.021	8.85

[a]GPC in water from nonsulfated PG polymers. [b]By elemental analysis. [c]By plaque reduction assay with sulfated polymers.

30 min. The cuvettes were prewarmed in the preincubation stand of the device for a minimum of 3 min.

Standard plasma (Siemens Healthcare ORKLI91E0005VM) was dissolved in 1 mL MQ water and was shaken gently at room temperature for 15 min. Steel stirrer balls, 50 μL of plasma solution, and 50 μL of actin FS (Siemens Healthcare OQTYI00E0009VM) were added to the cuvette. Upon addition of 2 μL of the inhibitor, the timer was started for the standard 180 s preincubation time. Thereafter, the cuvettes were transferred to the measurement stand of the instrument and the timer started by the addition of 50 μL of $CaCl_2$ solution with an electronic pipette. The time was automatically stopped by the formation of the clot. Each measurement was repeated three times.

RESULTS AND DISCUSSION

Design and Synthesis of Sulfated Inhibitors. Polymers were designed to mimic heparin, the naturally sulfated polysaccharide with a high density of negative charge. For synthesizing linear polyglycerol (LPG) and DenPGs, three different monomers were synthesized and polymerized via previously reported monomer-activated anionic ring-opening polymerization.[36] Hydroxy groups of the corresponding monomers were protected by an acetal group prior to polymerization, so that the polymer grows only in a linear structure and not in a hyperbranched one. Figure 1 shows the synthetic route for the monomer synthesis, polymerization, and then sulfation of polymers. The acetal protection of glycidol (1) was performed according to a previously reported protocol,[36] and two other monomers (6 and 10) were synthesized from the modification of solketal (5) and first-generation of dendritic PG (9) based on a slightly modified protocol for similar compounds, respectively (Figures S1−S3).[37] After polymerization, the acetal groups were deprotected to hydroxy groups in a slightly acidic environment (2, 5, 8).[36] The removal of acetal-protecting groups was monitored via ^{1}H NMR where the corresponding δ shift values at around 1.30 and 1.14 ppm disappeared. Three different polymers carrying one, two, or four hydroxy groups on each repeating unit were generated (Figures S1−S3). The polymer with one hydroxy group on the monomer (3) is a LPG. The other polymers with two (7) or four hydroxy groups (11) are referred to as dendronized polyglycerol generation 0.5 ($DenPG_{0.5}$) and dendronized polyglycerol generation ($DenPG_1$), respectively. The values 0.5 and 1 represent the generation of glycerol dendron on each repeating unit.[39]

Polymers were synthesized to carry the same number of −OH groups. Therefore, they have different degrees of polymerization. Based on their $\overline{M}_n$ (GPC, Table 1), LPG (3), $DenPG_{0.5}$ (7), and DenPG1 (11) have 239, 127, and 50 repeating units, respectively and therefore 239, 254, and 200 number of −OH groups, considering their polydispersity (PDI) values and their chain length, the difference in number of −OH groups is negligible, and these experimental values are in good agreement with theoretical ones. hPG was synthesized based on a reported protocol by our group.[40] The average molecular weight and PDI of different polymers are reported in Table 1.

Thereafter, all PGs were sulfated with a sulfur trioxide pyridine complex (SO_3·Py) based on a slightly modified previously reported protocol.[41] The transformation of hydroxyl groups to sulfate groups was confirmed by ^{1}H NMR, IR, and elemental analysis. After sulfation, the observed downfield shift of hydrogens next to sulfate groups in ^{1}H NMR (Figures S1−S3) and the appearance of a new band at 1200 cm^{-1} in IR spectroscopy (Figure S5) confirmed a successful sulfation. Furthermore, elemental analysis (CHNS) proved a high degree of sulfation for all sulfated compounds (Table 1). The surface charge of the polymers after sulfation was characterized by zeta(ζ) potential. The samples were measured at a concentration of 1 mg/mL in 10 mM PB (pH 7.4). All PGs displayed a high negative charge ranging from −26 mV for LPGS to −31 mV for DenPG1S. ζ-potential of commercially available heparin with a molecular weight of 13−15 kDa was −20.05 mV under the same conditions. The results are summarized in Table 1.

Cytotoxicity Studies. In order to investigate the potential of these new sulfated polymers to be safely applied as an anti-HSV-1 treatment in humans, their cytotoxicity was analyzed with the CCK-8 as the first step with the cell viability assay. For the test, two human lungs cell lines A549 and 16HBE14o were used as well as the Vero E6, the standard cell line used for infection assays and virus propagation. It was observed that upon treating the cells with sulfated compounds, cell viability was only slightly decreased upon treatment with LPGS and DenPGSs and up to a concentration of 1 mg/mL. No cytotoxicity was observed in any of the cell lines for none of the samples. This indicates that different cells could tolerate sulfated polymers up to a high concentration of 1 mg/mL (Figure S6).

Inhibition of HSV-1 Infection. After confirming that the different sulfated polymers did not reduce the cell viability up to relatively high concentrations, their antiviral activity against HSV-1 was investigated via the plaque reduction assay. The compounds were diluted in medium (10-fold dilutions) and then incubated with HSV-1 solution (approx. 200 PFU) for 45 min at 37 °C. The number of infectious viruses was then titrated on Vero E6 cells after the incubation with the compounds. The resulting curves are shown in Figure 2, and the IC_{50} values of the polymers are summarized in Table 1. All sulfated PGs effectively inhibited further infection of the cells, although with different activities. LPGS had the highest inhibitory activity with an IC_{50} value of 0.03 nM (0.0016 ± 0.0005 μg/mL). $DenPG_{0.5}S$ and $DenPG_1S$ were observed with IC_{50} values of 1.52 nM (0.049 ± 0.009 μg/mL) and 3.53 nM (0.072 ± 0.021 μg/mL), respectively, which reflects a lower activity than the LPGS but was higher than the hPGS (374.17 nM, 3.405 ± 1.14 μg/mL). As all inhibitors have similar overall

https://dx.doi.org/10.1021/acs.biomac.0c01789
Biomacromolecules 2021, 22, 1545−1554

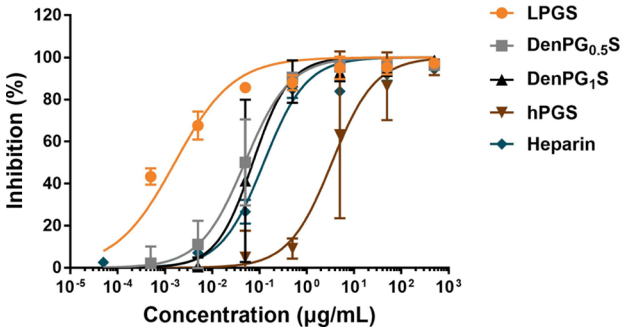

Figure 2. Dose−response curves of potential HSV-1inhibitors. The inhibitors were applied in serial dilutions to a solution containing app. 200 infectious HSV-1 particles (~200 PFU). Infectivity of the virus solution after incubating with the inhibitors was assessed by a plaque reduction assay using Vero E6 cells and is shown as a percentage of virus inhibition compared to HSV-1-containing control solution not treated with an inhibitor. Values are expressed as mean ± SD, n = 3.

degree of sulfation, this effect can be due to their different backbone flexibility. LPGS has a more flexible structure in comparison to the dendronized compounds which carry a half or first-generation glycerol dendron on each monomer unit. Furthermore, sulfated polymers with a linear LPG backbone are more flexible and, thus, could better adapt onto the virus surface than the relatively rigid hPGS polymer. This is in line with one of our previous studies on influenza A virus inhibition where high steric shielding contribution was observed and the optimized sialylated LPG polymer outperformed the dendritic analogue.[42] A clear relationship between the topology of the scaffold and the antiviral activity has been observed in carbosilane-based dendrimers against HIV infection as well.[43] In another study, it was observed that the dumbbell-shaped scaffolds have higher inhibitory activity against influenza virus than the ball- and fan-shaped ones.[44]

Alongside with synthesized inhibitors, commercially available heparin as a standard and natural virus inhibitor was tested in the same assay. The IC_{50} value of heparin (8.85 nM, 0.124 ± 0.021 μg/mL) was found to be higher than those of LPGS, $DenPG_{0.5}S$, and $DenPG_1S$, but lower than hPGS. This again highlights the dependence of inhibitory property on the structural flexibility of the inhibitors. hPGS with a globular structure is less flexible than heparin with a linear structure.

Afterward, the inhibition of the viral replication was studied in cellular infection assays. To investigate if the compounds can be used prophylactically, cells were incubated with the compounds at the concentration of 10 μg/mL for 45 min. Cells were then infected with HSV-1_GFP at a MOI of 0.1 for 48 h, which we call the preinfection application. During this time, the viral load reached 1×10^7 PFU/mL, which is much higher than the amount needed for plaque reduction assay. Therefore, in pre- and postinfection studies, higher concentration (10 μg/mL) was needed to achieve an effective inhibition.

Infection was studied by observing the infected cells and virus propagation by a plaque assay, as shown in Figure 3. LPGS and DenPGS showed one order of magnitudes higher activity for virus reduction and outperformed hPGS and heparin.

To study if the inhibitors would be effective after the virus has entered the cells, an assay was performed in a postinfection setup. This time, cells were first infected at a MOI of 0.1 for 45 min and then treated in the presence of the compounds for 48 h. The infection was studied by observing the infected cells and titrating the infectious virus in the medium. The same trend as in the preinfection incubation was observed for LPGS and DenPGSs against hPGS and heparin against HSV-1. In this case, a clear reduction of the number of infected cells and virus titer was noticed for LPGS and DenPGSs, indicating that the compound can effectively inhibit the infection of progeny virus after infection, thus reducing virus transmission. Heparin showed no activity in this assay, while LPGS and DenPGSs outperformed hPGS (Figure 3). By increasing the concentration to 100 μg/mL in this assay, a 4 log decrease in the number of cells was observed for LPGS and DenPGSs (Supporting Information-Figure S8). In this concentration, hPGS and heparin showed activity which was expected considering the fact that their IC_{50} values are much lower than 100 μg/mL.

LPGS as the most potent inhibitor was chosen to be compared with ACV as the standard medication for HSV-1 inhibition.[45] LPGS and ACV were compared in the both pre- and postinfection setups. In the preinfection study, at concentrations of 10 and 1 μM, LPGS performed slightly

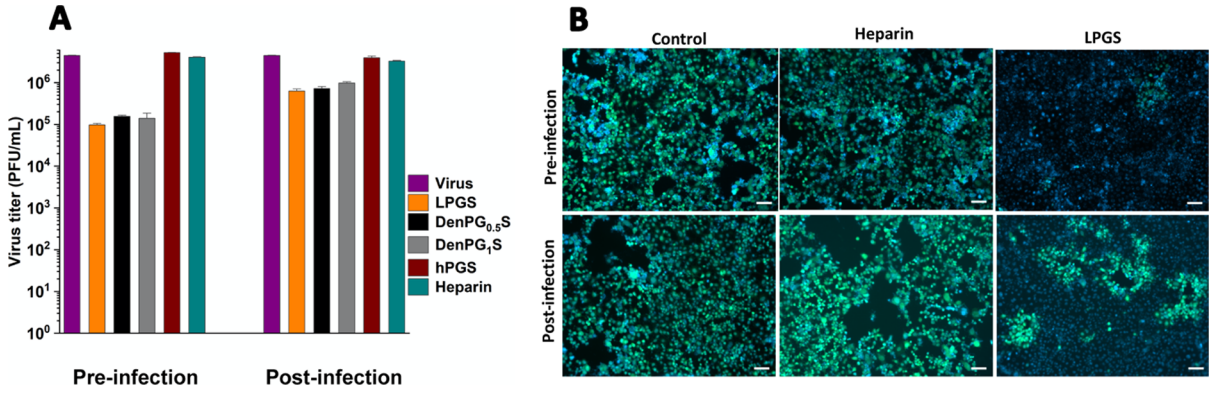

Figure 3. Inhibition of infection by pre- and postinfection treatment with compounds. Preinfection refers to adding the compounds to the cells before infecting the cells with HSV-1 and postinfection refers to the addition of compounds to the already infected cells. (A) Virus titers after treatment with 10 μg/mL of inhibitors (B) corresponding fluorescent microscopy images of the infected cells. Microscopy images from cells treated with other compounds are shown in Figure S7. Scale bar: 100 μm. Values are expressed as mean ± SD, n = 4. Total cells are marked blue for cell nuclei and the infected cells are marked green by GFP.

https://dx.doi.org/10.1021/acs.biomac.0c01789
Biomacromolecules 2021, 22, 1545−1554

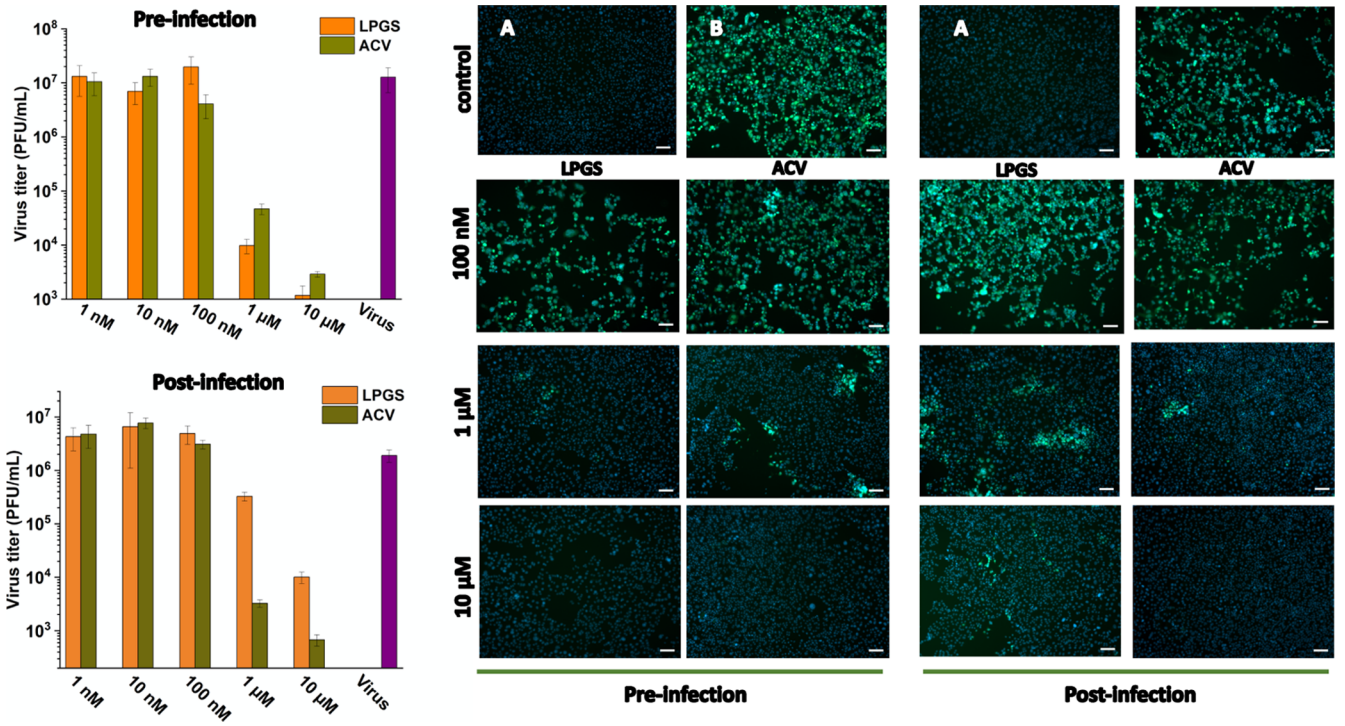

Figure 4. Quantitative virus titration of pre- and postinfection assays for LPGS and ACV and fluorescence microscopy images. (A, B are the noninfected and infected cells as control, respectively). Microscopy images from other concentrations are shown in Figure S9. Values are expressed as mean ± SD, n = 4. Scale bar: 100 μm. Total cells are marked blue for cell nuclei and the infected cells are marked green by GFP. A table with concentration conversion from nM to μg/mL can be found in Table S3.

better than ACV in inhibiting the virus entry and consecutively the viral infection. This trend was expected as LPGS is a HS mimetic and can interact with the virus surface and prevent it from interacting with the cell surface. At lower concentrations from 100 to 1 nM, LPGS and ACV did not have any significant difference in infection inhibition and they both could not inhibit the viral entry effectively. However, it was observed that at higher concentrations (1−10 μM), ACV performed slightly better than LPGS in preventing virus replication. This is probably due to the different acting mechanisms. ACV acts directly on host cells, where it interacts with the thymidine kinase in the cell and can block viral DNA synthesis and replication, which means even if virions have entered the cell, ACV can still function at this postentry step.[45]

LPGS, on the other hand, acts by blocking HSV-1 virions, which might be less efficient when the virus has already entered the cells. Our results also point out that LPGS can neutralize the progeny virus and prevent viral transmission between cells, as there is significantly fewer infected cells and lower virus titer in treated versus nontreated cells. At a concentration of 1 μM, ACV decreased the virus titer by one log larger than LPGS. Taken together, we conclude from our results that LPGS is comparable to ACV as an HSV-1 inhibitor. Figure 4 shows the virus titration of the pre- and postinfection assays with ACV and LPGS as well as the corresponding microscopic images.

Heparin has been shown to prolong blood clotting time by activating antithrombin and transforming it to a fast inhibitor of blood clotting proteinases, which makes it unfavorable for the clinical application as an HSV-1 inhibitor.[46] Sulfated synthetic polymers have also been reported to exhibit anticoagulant activity.[25] Therefore, in order to study the potential side effects of LPGS and DenPGSs, the ex vivo clotting times of plasma treated with sulfated synthetic inhibitors and heparin were investigated via determination of the activated partial thromboplastin time (aPTT), as shown in Figure 5.

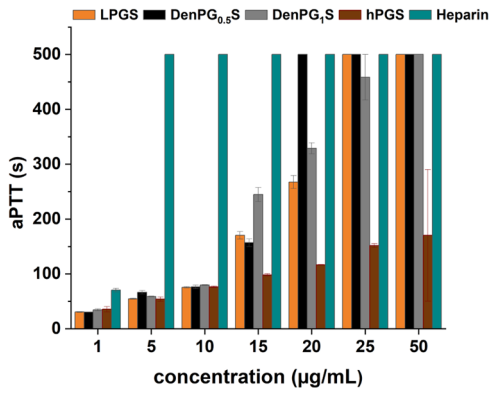

Figure 5. aPTT of synthetic inhibitors and heparin. Untreated human plasma with an aPTT of 31 s was used as a control. Values are expressed as mean ± SD, n = 3.

An increase in clotting times implies an increase of anticoagulant activity meaning the samples inhibit the formation of fibrinogen to insoluble fibrin for clot formation.[47] Untreated standard human plasma with an aPTT of 31 s was used as a control for this assay. The test was performed at different concentrations from 1 to 50 μg/mL. At a concentration of 1 μg/mL, inhibitors had no significant influence on the coagulation time in comparison to the untreated human plasma, while heparin increased the coagulation time up to two times at this concentration. At a

https://dx.doi.org/10.1021/acs.biomac.0c01789
Biomacromolecules 2021, 22, 1545−1554

concentration of 5 μg/mL, a moderate increase in the coagulation time for sulfated synthetic polymers was observed, while at this concentration, heparin increased the coagulation time to more than 16-fold. From 20 μg/mL, $DenPG_{0.5}S$ delayed the coagulation time to more than 500 s similar to heparin but LPGS and $DenPG_1S$ still increased the clotting time only up to 10-fold at the same concentration. At high concentrations (from 25 μg/mL), no difference between the DenPGS compounds and heparin was observed. hPGS delayed the clotting time up to a maximum of 50-fold over the control at 50 μg/mL. This strong difference of the effect of hPGS on the coagulation time in comparison to other inhibitors and heparin can likely be attributed to a more globular structure of the compound. Heparin with a linear structure has been shown to be a stabilizer for the thrombin−antithrombin complex and delays the blood coagulation.[46] The structures of linear and dendronized inhibitors are more similar to heparin than that of the of hPGS structure. Overall, sulfated PGs are much less anticoagulant than heparin, which is a significant advantage of the compounds synthesized and tested here, as unwanted bleeding as a treatment side effect is of considerable concern. Although hPGS has an advantage over LPGS and DenPGSs in regard to anticoagulant activity, it should be noted that LPGS and DenPGSs still have much lower IC_{50} values than hPGS. LPGS and DenPGSs have similar anticoagulant activities as dPGS up to 10 μg/mL. Therefore, based on our experiments, the linear scaffolds, specifically LPGS, are better antiviral candidates for future developments.

CONCLUSIONS

In this work, we have shown that the inhibitory potential of synthetic polymers against HSV-1 depends on their structure and flexibility. We designed and synthesized three different PG sulfate structures including linear, dendronized, and hyperbranched architectures. These polymers showed no acute cytotoxicity and were then tested for their antiviral activity against HSV-1 in comparison to heparin. The LPGS as the more flexible scaffold had a very low IC_{50} value in the pM range, and by adding bulky moieties to the scaffold (e.g., dendronized PG units) or engineering a globular structure such as hPGS, the IC_{50} values shift to higher numbers, highlighting the importance of polymer backbone flexibility for virus inhibition. To investigate potential antiviral activities of the compounds before and after infection, the samples were tested in pre- and postinfection assays. In both the assays, the linear inhibitors performed more efficiently than hPGS and heparin. The most effective compound, LPGS, was then compared with ACV and showed a comparable activity at concentrations above 1 μM in a preinfection assay. In the postinfection assay at the same concentration, although LPGS could effectively reduce the number of infected cells, ACV performed more efficiently as its mechanism of action is different than that of LPGS in this assay. Furthermore, it was observed that LPGS is a significantly better inhibitor than heparin, while having a lower anticoagulant activity. It can be concluded that LPGS is comparable to ACV as an HSV-1 inhibitor for infection prevention while acting via blocking virus entry and hence relying on a completely different mechanism.

ASSOCIATED CONTENT

Supporting Information

The Supporting Information is available free of charge at https://pubs.acs.org/doi/10.1021/acs.biomac.0c01789.

^1H NMR and ^{13}C NMR from monomer synthesis to sulfated polymer for linear and dendritic PG, ^1H NMR and ^{13}C NMR of hPG, GPC elugrams of synthesized inhibitors, IR spectra of polymers before and after sulfation, molecular weight of sulfated inhibitors from GPC, elemental analysis before and after sulfation of inhibitors, cell viability graphs, fluorescence microscopy images of pre- and postinfection assay for dendritic and hyperbranched PGs, virus titers after treatment with 100 μg/mL of inhibitors, and fluorescence microscopy images of pre- and postinfection assay of LPGS and ACV in 1 and 10 nM (PDF)

AUTHOR INFORMATION

Corresponding Author

Rainer Haag − *Institute of Chemistry and Biochemistry, Freie Universität Berlin, Berlin 14195, Germany;* orcid.org/0000-0003-3840-162X; Email: haag@chemie.fu-berlin.de

Authors

Paria Pouyan − *Institute of Chemistry and Biochemistry, Freie Universität Berlin, Berlin 14195, Germany*

Chuanxiong Nie − *Institute of Chemistry and Biochemistry and Institut für Virologie, Robert von Ostertag-Haus, Zentrum für Infektionsmedizin, Freie Universität Berlin, Berlin 14195, Germany*

Sumati Bhatia − *Institute of Chemistry and Biochemistry, Freie Universität Berlin, Berlin 14195, Germany*

Stefanie Wedepohl − *Institute of Chemistry and Biochemistry, Freie Universität Berlin, Berlin 14195, Germany*

Katharina Achazi − *Institute of Chemistry and Biochemistry, Freie Universität Berlin, Berlin 14195, Germany*

Nikolaus Osterrieder − *Institut für Virologie, Robert von Ostertag-Haus, Zentrum für Infektionsmedizin, Freie Universität Berlin, Berlin 14163, Germany; Department of Infectious Diseases and Public Health, Jockey Club College of Veterinary Medicine and Life Sciences, City University of Hong Kong, Kowloon Tong TYB-1B-507, Hong Kong*

Complete contact information is available at: https://pubs.acs.org/10.1021/acs.biomac.0c01789

Notes

The authors declare no competing financial interest.

ACKNOWLEDGMENTS

The authors would like to acknowledge the Core Facility BioSupraMol for assistance with NMR and MS measurements. The authors gratefully acknowledge financial support from German Research Foundation (DFG) through grants from the Collaborative Research Center (SFB) 765 and Federal Ministry of Education and Research (BMBF). We also would like to thank Dr. Pamela Winchester for proofreading the manuscript.

REFERENCES

(1) Bradshaw, M. J.; Venkatesan, A. Herpes Simplex Virus-1 Encephalitis in Adults: Pathophysiology, Diagnosis, and Management. *Neurotherapeutics* **2016**, *13*, 493−508.

(2) Katarzyna, K.; Aneta, P.; Anna, K.; Maria, N. Acyclovir in the Treatment of Herpes Viruses − A Review. *Curr. Med. Chem.* **2020**, *27*, 4118−4137.
(3) Laine, R. F.; Albecka, A.; van de Linde, S.; Rees, E. J.; Crump, C. M.; Kaminski, C. F. Structural analysis of herpes simplex virus by optical super-resolution imaging. *Nat. Commun.* **2015**, *6*, 5980.
(4) Balasubramaniam, R.; Kuperstein, A. S.; Stoopler, E. T. Update on Oral Herpes Virus Infections. *Dent. Clin. North Am.* **2014**, *58*, 265−280.
(5) Giraldo, D.; Wilcox, D. R.; Longnecker, R. The Innate Immune Response to Herpes Simplex Virus 1 Infection Is Dampened in the Newborn Brain and Can Be Modulated by Exogenous Interferon Beta To Improve Survival. *mBio* **2020**, *11*, No. e00921.
(6) Olsson, J.; Lövheim, H.; Honkala, E.; Karhunen, P. J.; Elgh, F.; Kok, E. H. HSV presence in brains of individuals without dementia: the TASTY brain series. *Dis. Models Mech.* **2016**, *9*, 1349−1355.
(7) Farooq, A. V.; Shukla, D. Herpes Simplex Epithelial and Stromal Keratitis: An Epidemiologic Update. *Surv. Ophthalmol.* **2012**, *57*, 448−462.
(8) Liu, Z.-h.; Niu, F.-j.; Xie, Y.-x.; Xie, S.-m.; Liu, Y.-n.; Yang, Y.-y.; Zhou, C.-z.; Wan, X.-h. A review: Natural polysaccharides from medicinal plants and microorganisms and their anti-herpetic mechanism. *Biomed. Pharmacother.* **2020**, *129*, 110469.
(9) Strasfeld, L.; Chou, S. Antiviral drug resistance: mechanisms and clinical implications. *Infect. Dis. Clin.* **2010**, *24*, 413−437.
(10) Bacon, T. H.; Levin, M. J.; Leary, J. J.; Sarisky, R. T.; Sutton, D. Herpes Simplex Virus Resistance to Acyclovir and Penciclovir after Two Decades of Antiviral Therapy. *Clin. Microbiol. Rev.* **2003**, *16*, 114.
(11) Soria-Martinez, L.; Bauer, S.; Giesler, M.; Schelhaas, S.; Materlik, J.; Janus, K.; Pierzyna, P.; Becker, M.; Snyder, N. L.; Hartmann, L.; Schelhaas, M. Prophylactic Antiviral Activity of Sulfated Glycomimetic Oligomers and Polymers. *J. Am. Chem. Soc.* **2020**, *142*, 5252−5265.
(12) Sarrazin, S.; Lamanna, W. C.; Esko, J. D. Heparan sulfate proteoglycans. *Cold Spring Harbor Perspect. Biol.* **2011**, *3*, a004952.
(13) Shieh, M. T.; WuDunn, D.; Montgomery, R. I.; Esko, J. D.; Spear, P. G. Cell surface receptors for herpes simplex virus are heparan sulfate proteoglycans. *J. Cell Biol.* **1992**, *116*, 1273−1281.
(14) Bartlett, A. H.; Park, P. W. Proteoglycans in host−pathogen interactions: molecular mechanisms and therapeutic implications. *Expert Rev. Mol. Med.* **2010**, *12*, No. e5.
(15) Ma, G.; Azab, W.; Osterrieder, N. Equine herpesviruses type 1 (EHV-1) and 4 (EHV-4)—Masters of co-evolution and a constant threat to equids and beyond. *Vet. Microbiol.* **2013**, *167*, 123−134.
(16) Pachota, M.; Klysik, K.; Synowiec, A.; Ciejka, J.; Szczubiałka, K.; Pyrć, K.; Nowakowska, M. Inhibition of Herpes Simplex Viruses by Cationic Dextran Derivatives. *J. Med. Chem.* **2017**, *60*, 8620−8630.
(17) Pachota, M.; Kłysik-Trzciańska, K.; Synowiec, A.; Yukioka, S.; Yusa, S.-I.; Zając, M.; Zawilinska, B.; Dzieciątkowski, T.; Szczubialka, K.; Pyrc, K.; Nowakowska, M. Highly Effective and Safe Polymeric Inhibitors of Herpes Simplex Virus in Vitro and in Vivo. *ACS Appl. Mater. Interfaces* **2019**, *11*, 26745−26752.
(18) Xia, T.; Rome, L.; Nel, A. Particles slip cell security. *Nat. Mater.* **2008**, *7*, 519−520.
(19) Jarach, N.; Dodiuk, H.; Kenig, S. Polymers in the Medical Antiviral Front-Line. *Polymers* **2020**, *12*, 1727.
(20) Bianculli, R. H.; Mase, J. D.; Schulz, M. D. Antiviral Polymers: Past Approaches and Future Possibilities. *Macromolecules* **2020**, *53*, 9158−9186.
(21) Yadavalli, T.; Mallick, S.; Patel, P.; Koganti, R.; Shukla, D.; Date, A. A. Pharmaceutically Acceptable Carboxylic Acid-Terminated Polymers Show Activity and Selectivity against HSV-1 and HSV-2 and Synergy with Antiviral Drugs. *ACS Infect. Dis.* **2020**, *6*, 2926−2937.
(22) Richards, K. F.; Bienkowska-Haba, M.; Dasgupta, J.; Chen, X. S.; Sapp, M. Multiple heparan sulfate binding site engagements are required for the infectious entry of human papillomavirus type 16. *J. Virol.* **2013**, *87*, 11426−11437.
(23) Nahmias, A. J.; Kibrick, S. Inhibitory effect of heparin on herpes simplex virus. *J. Bacteriol.* **1964**, *87*, 1060−1066.
(24) Oduah, E.; Linhardt, R.; Sharfstein, S. Heparin: Past, Present, and Future. *Pharmaceuticals* **2016**, *9*, 38.
(25) Paluck, S. J.; Nguyen, T. H.; Maynard, H. D. Heparin-Mimicking Polymers: Synthesis and Biological Applications. *Biomacromolecules* **2016**, *17*, 3417−3440.
(26) Achazi, K.; Haag, R.; Ballauff, M.; Dernedde, J.; Kizhakkedathu, J. N.; Maysinger, D.; Multhaup, G. Understanding the Interaction of Polyelectrolyte Architectures with Proteins and Biosystems. *Angew. Chem., Int. Ed.* **2021**, *60*, 3882−3904.
(27) Imran ul-haq, M.; Lai, B. F. L.; Chapanian, R.; Kizhakkedathu, J. N. Influence of architecture of high molecular weight linear and branched polyglycerols on their biocompatibility and biodistribution. *Biomaterials* **2012**, *33*, 9135−9147.
(28) Haag, R.; Kratz, F. Polymer Therapeutics: Concepts and Applications. *Angew. Chem., Int. Ed.* **2006**, *45*, 1198−1215.
(29) Türk, H.; Haag, R.; Alban, S. Dendritic Polyglycerol Sulfates as New Heparin Analogues and Potent Inhibitors of the Complement System. *Bioconjugate Chem.* **2004**, *15*, 162−167.
(30) Dernedde, J.; Rausch, A.; Weinhart, M.; Enders, S.; Tauber, R.; Licha, K.; Schirner, M.; Zügel, U.; von Bonin, A.; Haag, R. Dendritic polyglycerol sulfates as multivalent inhibitors of inflammation. *Proc. Natl. Acad. Sci. U.S.A.* **2010**, *107*, 19679.
(31) Sametband, M.; Kalt, I.; Gedanken, A.; Sarid, R. Herpes Simplex Virus Type-1 Attachment Inhibition by Functionalized Graphene Oxide. *ACS Appl. Mater. Interfaces* **2014**, *6*, 1228−1235.
(32) Ziem, B.; Azab, W.; Gholami, M. F.; Rabe, J. P.; Osterrieder, N.; Haag, R. Size-dependent inhibition of herpesvirus cellular entry by polyvalent nanoarchitectures. *Nanoscale* **2017**, *9*, 3774−3783.
(33) Donskyi, I. S.; Azab, W.; Cuellar-Camacho, J. L.; Guday, G.; Lippitz, A.; Unger, W. E. S.; Osterrieder, K.; Adeli, M.; Haag, R. Functionalized nanographene sheets with high antiviral activity through synergistic electrostatic and hydrophobic interactions. *Nanoscale* **2019**, *11*, 15804−15809.
(34) Bhatia, S.; Hilsch, M.; Cuellar-Camacho, J. L.; Ludwig, K.; Nie, C.; Parshad, B.; Wallert, M.; Block, S.; Lauster, D.; Böttcher, C.; Herrmann, A.; Haag, R. Adaptive Flexible Sialylated Nanogels as Highly Potent Influenza A Virus Inhibitors. *Angew. Chem., Int. Ed.* **2020**, *59*, 12417−12422.
(35) Alpugan, S.; Garcia, G.; Poyer, F.; Durmuş, M.; Maillard, P.; Ahsen, V.; Dumoulin, F. Dendrimeric-like hexadecahydroxylated zinc phthalocyanine: Synthesis and evaluation of photodynamic efficiency. *J. Porphyrins Phthalocyanines* **2013**, *17*, 596−603.
(36) Gervais, M.; Brocas, A.-L.; Cendejas, G.; Deffieux, A.; Carlotti, S. Synthesis of Linear High Molar Mass Glycidol-Based Polymers by Monomer-Activated Anionic Polymerization. *Macromolecules* **2010**, *43*, 1778−1784.
(37) Geschwind, J.; Frey, H. Stable, Hydroxyl Functional Polycarbonates With Glycerol Side Chains Synthesized From CO2 and Isopropylidene(glyceryl glycidyl ether). *Macromol. Rapid Commun.* **2013**, *34*, 150−155.
(38) Young, L.; Sung, J.; Stacey, G.; Masters, J. R. Detection of Mycoplasma in cell cultures. *Nat. Protoc.* **2010**, *5*, 929−934.
(39) Wyszogrodzka, M.; Haag, R. Study of Single Protein Adsorption onto Monoamino Oligoglycerol Derivatives: A Structure−Activity Relationship. *Langmuir* **2009**, *25*, 5703−5712.
(40) Sunder, A.; Hanselmann, R.; Frey, H.; Mülhaupt, R. Controlled Synthesis of Hyperbranched Polyglycerols by Ring-Opening Multibranching Polymerization. *Macromolecules* **1999**, *32*, 4240−4246.
(41) Ferraro, M.; Silberreis, K.; Mohammadifar, E.; Neumann, F.; Dernedde, J.; Haag, R. Biodegradable Polyglycerol Sulfates Exhibit Promising Features for Anti-inflammatory Applications. *Biomacromolecules* **2018**, *19*, 4524−4533.
(42) Bhatia, S.; Lauster, D.; Bardua, M.; Ludwig, K.; Angioletti-Uberti, S.; Popp, N.; Hoffmann, U.; Paulus, F.; Budt, M.; Stadtmüller, M.; Wolff, T.; Hamann, A.; Böttcher, C.; Herrmann, A.; Haag, R. Linear polysialoside outperforms dendritic analogs for inhibition of influenza virus infection in vitro and in vivo. *Biomaterials* **2017**, *138*, 22−34.

https://dx.doi.org/10.1021/acs.biomac.0c01789
Biomacromolecules 2021, 22, 1545−1554

(43) Gutierrez-Ulloa, C. E.; Sepúlveda-Crespo, D.; García-Broncano, P.; Malý, M.; Muñoz-Fernández, M. A.; de la Mata, F. J.; Gómez, R. Synthesis of bow-tie carbosilane dendrimers and their HIV antiviral capacity: A comparison of the dendritic topology on the biological process. *Eur. Polym. J.* **2019**, *119*, 200−212.
(44) Hatano, K.; Matsubara, T.; Muramatsu, Y.; Ezure, M.; Koyama, T.; Matsuoka, K.; Kuriyama, R.; Kori, H.; Sato, T. Synthesis and Influenza Virus Inhibitory Activities of Carbosilane Dendrimers Peripherally Functionalized with Hemagglutinin-Binding Peptide. *J. Med. Chem.* **2014**, *57*, 8332−8339.
(45) Rabelo, V. W.-H.; Romeiro, N. C.; Paixão, I. C. N. d. P.; Abreu, P. A. Mechanism of resistance to acyclovir in thymidine kinase mutants from Herpes simplex virus type 1: a computational approach. *J. Biomol. Struct. Dyn.* **2020**, *38*, 2116−2127.
(46) Olson, S. T.; Richard, B.; Izaguirre, G.; Schedin-Weiss, S.; Gettins, P. G. W. Molecular mechanisms of antithrombin-heparin regulation of blood clotting proteinases. A paradigm for understanding proteinase regulation by serpin family protein proteinase inhibitors. *Biochimie* **2010**, *92*, 1587−1596.
(47) Huang, Y.; Shaw, M. A.; Mullins, E. S.; Kirley, T. L.; Ayres, N. Synthesis and anticoagulant activity of polyureas containing sulfated carbohydrates. *Biomacromolecules* **2014**, *15*, 4455−4466.

https://dx.doi.org/10.1021/acs.biomac.0c01789
Biomacromolecules 2021, 22, 1545−1554